Engineering Notes

ENGINEERING NOTES are short manuscripts describing new developments or important results of a preliminary nature. These Notes cannot exceed 6 manuscript pages and 3 figures; a page of text may be substituted for a figure or vice versa. After informal review by the editors, they may be published within a few months of the date of receipt. Style requirements are the same as for regular contributions (see inside back cover).

An Experimental Investigation of Base Heating on Typical Mars Entry Body Shapes

O. L. ZAPPA* AND W. G. REINECKE†
Avco Systems Division, Wilmington, Mass.

Nomenclature

D = maximum model diameter
g_w = wall to freestream stagnation enthalpy ratio
M = Mach number
P = pressure
$\dot{q}$ = local heat-transfer rate
$\dot{q}_0$ = reference stagnation point heating rate for sphere of diameter D
$\dot{q}_{Bo}$ = reference base heating rate
R_B, R_N = base, nose radius of model
$R_{\infty,D}$ = Reynolds number based on model diameter and freestream conditions
v = velocity
γ = ratio of specific heats
ρ = density
μ = viscosity
χ = defined in Fig. 1

Subscripts

b = base
∞ = freestream conditions
e = boundary edge conditions

Introduction

THE consideration of probe/lander entry into the tenuous Martian atmosphere in conjunction with the Viking mission constraints and requirements has resulted in the selection of high-drag shapes with relatively large afterbodies. The heating rates over these large-area bases must be determined in order to determine the weight of the required thermal protection. Unfortunately, of the many viscous flow problems associated with hypersonic vehicles, the separated flow region, particularly the base region, is the least understood, and empirical relations are necessary to predict the separation characteristics.[1] In particular, the correlation of the base heating is complicated by the entropy variation along the boundary-layer edge, which involves a coupled boundary-layer flowfield solution. Early analyses of the viscous flow phenomena over a planetary probe entering the Martian atmosphere[2] indicated the importance of variable entropy considerations in evaluating the forebody heating distributions at the flight conditions associated with peak laminar heating. This varying boundary-layer edge also influences the heating in the base region since the flow conditions prior to expansion into the wake are altered. These complications indicate that in order to assist in the engineering prediction of the heating environment, it is necessary to determine experimentally the heating in the base region. The present study was undertaken to obtain such heating data. Effects of variations in the base geometry were considered, as well as the influences of the forebody.

Presented as Paper 72-317 at AIAA 7th Thermophysics Conference, San Antonio, Texas, April 10–12, 1972; submitted March 30, 1972; revision received November 13, 1972. This research was supported by Contract NAS1-9368, NASA, Washington, D. C.

Index categories: Entry Vehicles and Landers; Boundary Layers and Convective Heat Transfer—Laminar; Jets, Wakes, and Viscid-Inviscid Flow Interactions.

* Senior Consulting Scientist.
† Senior Consulting Scientist. Associate Fellow AIAA.

Description of Experiments

The 20-inch-diam shock tunnel at Avco Systems Division was used for the tests described herein. The two test conditions were a Mach number of 11.5, a total temperature of 3000°R, and test section unit Reynolds numbers of 3.0×10^5 and 2.5×10^6 per foot.

Six different model geometries were tested in the course of the study. The first four models were 4-in.-diam, 60° half-angle cones with spherical noses of $\frac{1}{2}$-in. radius and 13° 31′ boattails. The fifth model was a 3-in.-diam sphere, and the sixth model was a 4-in.-diam, 70° half-angle cone, also spherically blunted with a 1-in. radius but with a 40° boattail. The first four models used a common forebody made of steel. The model geometry was altered by attaching one of four different aluminum afterbodies. The model was suspended in the tunnel by 4 steel cables 0.066 in. in diameter, which were attached directly to the tunnel sidewalls. The attachments on the model were on the forebody at points rotated 45° from the line of the thin-skinned heat-transfer gages (as seen from fore or aft) to minimize any possible interference effects. Since only two ports were available with which to vary the location of the cables at the shock tunnel wall to affect an angle-of-attack variation, an angle of roll between the gage plane and the pitch plane of 45° resulted. Additional tests were conducted with a mounting system which provided a true angle of attack in the heat-transfer gage plane.

Method of Correlation

The application of these ground test data to the evaluation of the base heating for flight conditions requires the use of suitable correlation parameters. An alternate approach is to select a basic or reference heating rate with which to normalize the data. The liklihood that the normalized heating ratio varies only slightly between test and flight makes this approach very desirable, particularly in the early stages of design. The reference heating rate selected was the stagnation-point heating for a sphere whose diameter is equal to that of the cones. This heating is readily evaluated with knowledge of the flight parameter histories. An insight into the variation of this normalized heating is obtainable by means of Reynolds number variation. This parameter is important since, in addition to being critical in terms of the base pressure extent, it also is indicative of the extent of entropy-layer swallowing in the forebody boundary layer.

An alternate reference heating rate was considered which included these variable entropy and base pressure effects. Correlations of the base pressure that were available required an extrapolation to lower Mach numbers. The two reference heating rates are discussed below. The above effects were more noticeable for the 120° cone since the larger nose radius and blunter cone angle resulted in a flatter shock wave for the 140° cone.

The sphere stagnation-point reference heating rate was obtained by measurements in the shock tunnel at freestream conditions comparable to those for the cone tests. The sting mounted hemisphere model used was tested at three Reynolds numbers at a Mach number of 11.5. The data was compared with an analytical prediction method,[3] the results of which are summarized in Table 1.

Table 1 Stagnation heating correlation

Reynolds no., $\rho_\infty V_\infty D/\mu_\infty$	53300	410000	620000
$\dot{q}_{test}/\dot{q}_{theory}$	0.94, 1.11	1.20	1.18

The dependence of the base pressure on the Reynolds number indicates a need for a normalizing heat-transfer rate which is a function of the base pressure. A possible reference heating rate that can be used is that determined by evaluating the heating associated with the base pressure assuming an ideal expansion from the forebody.

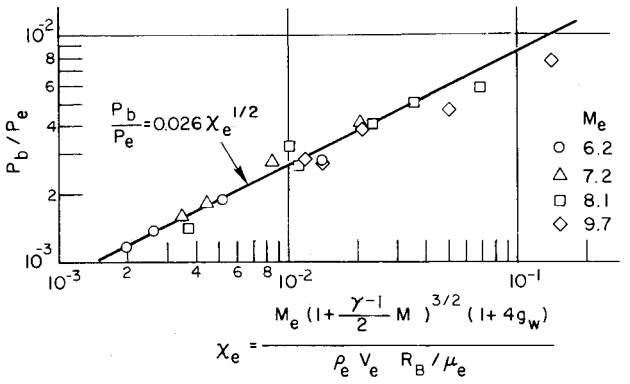

Fig. 1 Correlation of base pressure with experimental data.

Figure 1 presents a correlation obtained for sharp cones[1] based on local boundary-layer edge conditions prior to separation. The application of these data requires an extrapolation in order to utilize it for blunt cones. The mass swallowing in the boundary layer was computed iteratively[4] and the external flow characteristics determined at the maximum diameter region. The heating prior to separation as well as the reference base heating were computed by means of the reference enthalpy method.[4,5]

The variable entropy effects on the 140° cone were very small for the test conditions. Table 2 presents a tabulation of the reference heating rates for the two test Reynolds numbers for the 120° cone computed by the above method. The reference base values are less sensitive to Reynolds number than the stagnation point on the sphere since the base pressure decreases with Reynolds number.

120° Cone Results—Configurations 1 and 2

Configurations 1 and 2 data are presented together since both had the same geometry; the boattail angle and length were $13\frac{1}{2}°$ and 0.23 D, respectively. Configuration 1 had a flat base whereas configuration 2 had a conical-concave base. The configuration 1 data were obtained only at zero angle of attack. Figure 2 presents results for stations located in three regions of the afterbody, i.e., the boattail and the inner and outer base region. The inner base data (all the data have been normalized by means of the reference sphere stagnation point heating) indicated a reduced heating at angle of attack for both windward and leeward stations, whereas the outer stations exhibited higher heating for the leeward station. The boattail region exhibited attached-flow-type heating variations. It would be expected that the concave base would experience reduced heating at the axis of symmetry similar to concave nose shapes in stagnation-point flow. Figure 3 indicates this is possible for the base flow stagnation point; however, this is not apparent for the other base stations. There was very little difference in boattail heating between the two configurations. Only one test was conducted for the configuration 2 shape at a true angle of attack of 10° (low pressure). The results did not indicate a significant difference on trend in the heating between the out of pitch and the true pitch data.

The use of CO_2 gas mixtures as the test medium resulted in Reynolds numbers similar to the high Reynolds number for air as shown in Table 3. The data with the CO_2 mixtures (the flagged symbols in the figures) were consistent with the high Reynolds number air results.

Table 2 Reference heating values

$R_{\infty,D}$	1×10^5	0.83×10^6
Reference stagnation point heating on sphere, $R_N = 2$ in. (w/cm^2)	22.5	77.0
Reference base heating, $R_N = 2$ in. (w/cm^2)	1.5	2.7

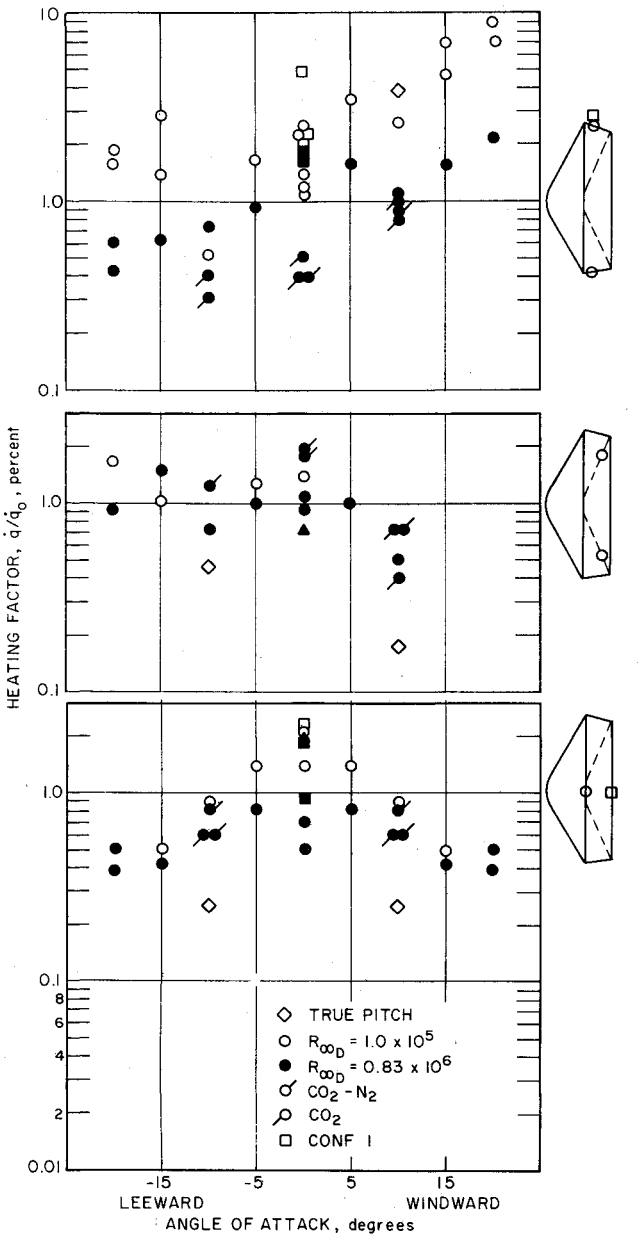

Fig. 2 Base heating, configuration 1 and 2—approximate gage locations indicated on insets.

Table 3 Reynolds number dependence on test mixture

Test mixture	Freestream Reynolds number per foot
Air	2.5×10^6
Carbon dioxide	1.74×10^6
80 CO_2/20 N_2	1.9×10^6

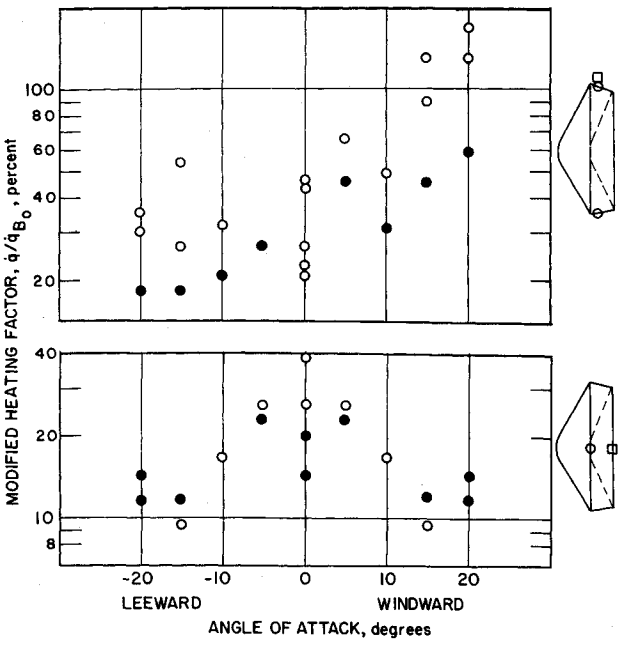

Fig. 3 Base heating configuration 2, modified factor—approximate gage locations indicated on insets.

Utilizing the base reference heating rates in lieu of the sphere stagnation-point heating for normalizing the data results generally in a reduction in the spread of the data between the two Reynolds numbers. In particular, the base region data (Fig. 2) agree reasonably well with this correlation. The level of heating is less than would be predicted by Chapman.[6] However, there is a Reynolds number effect for the boattail (Fig. 2) which is unaccounted for even by the base pressure dependency discussed above. Viscous interaction may be a possible source of these results.

120° Cone Results—Configurations 3 and 4

These configurations had the same boattail angle as models 1 and 2 ($13\frac{1}{2}°$) but had a shorter boattail (0.11 D long). Configuration 4 had in addition an appendage on the axis of symmetry (a cylinder of diam 0.18 D). Configuration 3 data were obtained only at zero angle of attack. The results were substantially the same as those for configurations 1 and 2. Within the basic regions defined above, i.e., boattail and inner and outer base, no definitive statement can be made with regard to the variation in heating among the shapes. The angle-of-attack variations were similar and the level of heating was the same for the configurations 3 and 4 and configurations 1 and 2.

140° Cone—Configuration 6

The Viking configuration exhibited the base flow heating characteristic (Fig. 4) similar to configurations 1–4, when considering the boattail as part of the base. The heating was higher on the leeward side (compare Fig. 4 with Fig. 2) in contrast to the windward side for the outer base region. The inner region of the Viking configuration did not exhibit the reduction in heating at angle of attack which characterized configurations 2 and 4. The base heating for the 140° cone was generally lower than the 120° cone. In addition there was less of a Reynolds number effect for the Viking shape in contrast to the other shapes. This is to be expected since the variable entropy effects are considerably less; however, the base pressure effect should still be apparent. The 140° cone results agree best with the high-Reynolds-number 120° cone results. It has been estimated that at the high-Reynolds-number test conditions, the 120° cone has normal shock entropy at the maximum diameter stations. Finally, note that the pitch plane and out-of-pitch

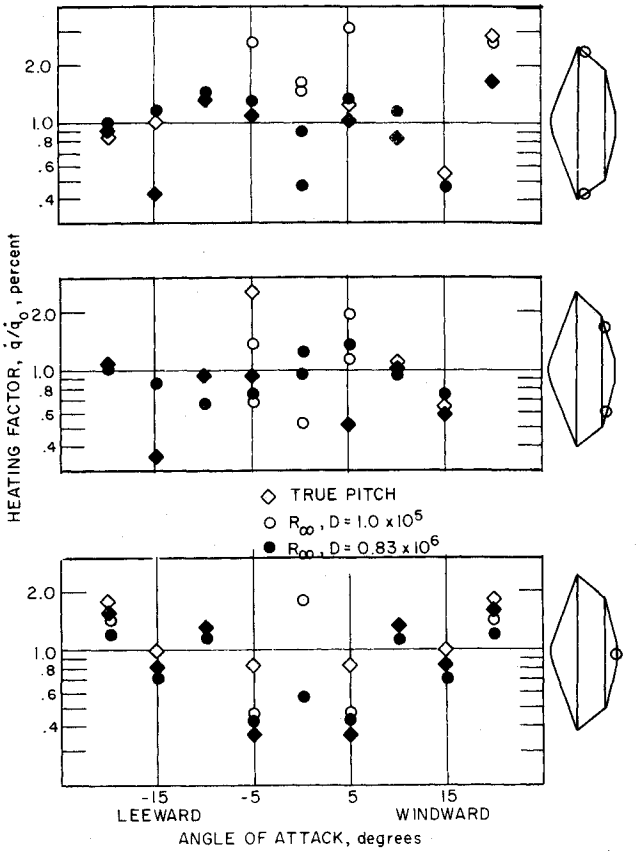

Fig. 4 Base heating configuration 6—approximate gage locations indicated on insets.

plane data are consistent within the scatter exhibited by the data.

Summary

The results of the present experimental investigation have indicated that the base heating rates are less than 2% for the Viking shape (140° cone) based on the reference sphere heating. The 120° cone base heating is slightly higher and more sensitive to Reynolds number. The use of a reference base heating results in a reduced variation in the data for variations in the Reynolds number. The average heating in the separated base region is less than would be predicted by Chapman.[6]

The boattail region experiences the highest heating, and has the usual variation with angle of attack, although the values measured were lower than were expected. The outer separated region experiences reduced heating on the windward side at angle of attack, whereas the inner separated region exhibited reduced heating for both the windward and the leeward side.

The variation in test gas mixture resulted in base heating which was consistent with the previous air data when compared with the proper Reynolds number. Variable entropy effects were similar since the shock shapes were comparable (the shock density ratios were equal).

A more extensive description of the experiments and correlation is given in Ref. 7.

References

[1] Reeves, B. L. and Buss, H. M., "Theory of the Laminar Near Wake of Axisymmetric Slender Bodies in Hypersonic Flow," AVMSD-0122-69-RR, Feb. 1969, Avco Missile Systems Div., Wilmington, Mass.

[2] "Comparative Studies of Conceptual Design and Qualification Procedures for a Mars Probe/Lander, Final Report," Vol. V, Book 2, AVSSD-0006-66-RR, May 1966, Space Systems Div., Lowell, Mass.

[3] Fay, J. A. and Riddell, F. R., "Theory of Stagnation Point Heat Transfer in Dissociated Air," Research Rept. 1, 1957, Avco Everett Research Lab., Everett, Mass.

[4] Schurmann, E. E. H., "Engineering Methods for the Analysis of Aerodynamic Heating (U)," RAD-TM-63-68, Nov. 1963, Avco, Wilmington, Mass.

[5] Eckert, E. R. G., "Survey on Heat Transfer at High Speeds," TR 56-70, April 1954, NADC.

[6] Chapman, D. R., "A Theoretical Analysis of Heat Transfer in Regions of Separated Flow," TN 3792, Oct. 1956, NACA.

[7] Zappa, O. L. and Reinecke, W. S., "An Experimental Investigation of Base Heating on Typical Mass Entry Body Shapes," CR-1920, Nov. 1971, NASA.

Relative Magnitudes of Stresses Caused by Static and Dynamic Launch Vehicle Loads

LARS E. ERICSSON,* J. PETER READING,† AND ROLF A. GUENTHER‡
Lockheed Missiles & Space Company Inc., Sunnyvale, Calif.

WHEN discussing elastic launch vehicle response to sinusoidal gusts,[1] one faces the problem of finding a suitable reference level which makes it possible for the reader to assess the seriousness of the gust response. This Note describes such a reference level based upon the comparison between the stresses occurring under static and dynamic loads. In Ref. 1, the amplitude $|\theta_N|_{max}$ of the launch vehicle tip, resulting from passage through sinusoidal gusts, was computed for the Saturn V booster. This amplitude generates certain maximum stresses in the vehicle. By comparing those gust-induced dynamic stresses with the stresses produced by the static loads at angle of attack α, one can determine an equivalent static angle of attack giving the same stress level as the dynamic gust response.

For simplicity, the cantilever-beam approximation is used for the launch vehicle deflection under load. With the definitions of Fig. 1, one obtains

$$y'' = \partial^2 y/\partial x^2 = -[M_b(x)/EI(x)] \tag{1}$$

Using the normalized bending mode formulation, the deflection can be written[1]

$$\left.\begin{aligned} y(x) &= q(t)\phi(x) \\ \theta_N &= q(t)\phi'(x_N) \\ y''(x) &= q(t)\phi''(x) \end{aligned}\right\} \tag{2}$$

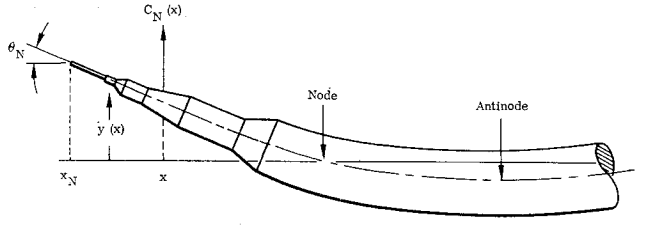

Fig. 1 Definition of elastic launch vehicle variables.

Received July 21, 1972.
Index categories: Rocket Vehicle Gust Loading and Wind shear; Nonsteady Aerodynamics; Aeroelasticity and Hydroelasticity.

* Senior Staff Engineer. Associate Fellow AIAA.
† Research Specialist. Member AIAA.
‡ Senior Aerodynamics Engineer.

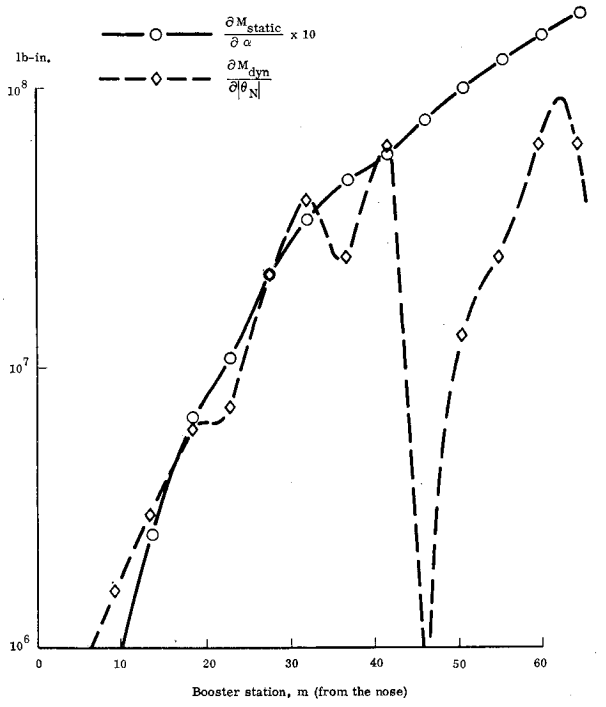

Fig. 2 Comparison of dynamic and static bending moments on Saturn V at maximum dynamic pressure, $M = 1.6$ (1st B.M.).

Thus

$$y''(x) = \phi''(x)\theta_N/\phi'(x_N) \tag{3}$$

and Eq. (1) becomes

$$|M_b(x)|_{dyn} = \left[\frac{\phi''(x)}{\phi'(x_N)}\right][EI(x)]\,|\theta_N| \tag{4}$$

The static bending moment at x is

$$\left.\begin{aligned} [M_b(x)]_{static} &= \left(\frac{\rho U^2}{2}\right) S\alpha \int_x^{x_N} \frac{dC_{N\alpha}}{dx}(x_N - x)dx \\ &= \left(\frac{\rho U^2}{2}\right) S\alpha \sum_{n=0}^{n} C_{N(\alpha_n)}(x_N - x_n) \end{aligned}\right\} \tag{5}$$

Using the structural parameters for Saturn V, mode shape $\phi(x)$ from Ref. 2, and inertia $I(x)$ from Ref. 3, the dynamic moment amplitude $|M_b(x)|_{dyn}$ defined by Eq. (4) has been computed. In Fig. 2 the dynamic moment amplitude for the first bending mode is compared with the static moment defined by Eq. (5). One can see that $|M_b(x)|_{dyn}$ for $|\theta_N| = 1°$ and $[M_b(x)]_{static}$ for $\alpha = 10°$ are of the same order of magnitude. The dynamic moment reaches maximum at the (first) antinode, the point of maximum curvature, and the computations need not be carried beyond this station in order to establish a reference α for the $|\theta_N|$-effect.

References

[1] Ericsson, L. E., Reding, J. P., and Guenther, R. A., "Elastic Launch Vehicle Response to Sinusoidal Gust," *Journal of Spacecraft and Rockets*, Vol. 10, No. 4, April 1973, pp. 244–252.

[2] Riley, G. F., "AS-507 Structural Damping Characteristics," Doc. D5-15541, Vol. II, Contract NAS 8-5608, Aug. 6, 1969, The Boeing Co., Seattle, Wash.

[3] Ivey, W. and Sims, J., "Vibration Analysis of the Saturn V Operational Vehicle," R-P&VE-SLA-64-11, April 10, 1964, NASA.